Electrochemical Studies on the Modular Podand 1,3,5-Tris(3-((ferrocenylmethyl)amino)pyridiniumyl)-2,4,6-triethylbenzene Hexafluorophosphate in Conventional Solvents and Ionic Liquids

Jie Zhang and Alan M. Bond*

School of Chemistry, P.O. Box 23, Monash University, Clayton, Victoria 3800, Australia

Warwick J. Belcher, Karl J. Wallace, and Jonathan W. Steed*

Department of Chemistry, King's College London, Strand, London WC2R 2LS, U.K.

Received: December 12, 2002; In Final Form: March 13, 2003

The solution-phase voltammetry of the modular podand, 1,3,5-tris(3-((ferrocenylmethyl)amino)pyridiniumyl)-2,4,6-triethylbenzene hexafluorophosphate, $[PD][PF_6]_3$, in acetonitrile (0.1 M Bu_4NPF_6) and the ionic liquids [1-butyl-3-methylimidazolium hexafluorophosphate, (ethylmethylimidazoliumyl)bis(trifluoromethylsulfonyl)-amide, and (*n*-butylmethylpyrrolidiniumyl)bis(trifluoromethylsulfonyl)amide] exhibits a well-defined diffusion-controlled process at a potential of about 1.40 V vs $[Co(\eta^5\text{-}C_5H_5)_2]^{+/0}$. Detailed chronoamperometric and near steady-state microdisk electrode studies reveal that although the process has many of the characteristics of a reversible one-electron oxidation reaction, it is actually a combination of three very closely spaced reversible one-electron processes, implying that there is minimal communication between the three ferrocenyl redox active centers present in the podand. The voltammetry of very slowly dissolving microparticles of $[PD][PF_6]_3$ mechanically attached to an electrode surface in contact with ionic liquids is indistinguishable from that observed when the podand is in the dissolved state in the ionic liquid. In contrast, cyclic voltammograms obtained when a $[PD][PF_6]_3$ modified electrode is in contact with aqueous electrolyte media exhibit behavior very different from that found in the solution phase. For example, in the presence of KPF_6 electrolyte, three resolved oxidation peaks are detected, whereas in some other electrolyte media, transformations to features expected in stripping voltammetry are encountered on repetitive cycling of the potential. Unlike the case in ionic liquids, $[PD][PF_6]_3$ is thermodynamically insoluble in water, although oxidized forms are believed to have an anion dependent level of solubility. Consequently, an oxidation−dissolution/reduction−reprecipitation and ion exchange type mechanism is believed to lead to a transition from the "thick" to "thin" film type of voltammetric behavior, which is supported by numerical simulation.

Introduction

The design and synthesis of host−guest systems is very important in the field of supramolecular chemistry[1,2] due to their potential applications in ion sensing and extraction.[1−14] On the basis of possibilities for anion sensing using spectroscopic probes, a range of ferrocene-containing modular podands (molecular clips) have been prepared.[6] Ferrocene derivatives are incorporated into the molecular design in the hope of observing a change in the well-known metallocene redox properties upon anion binding. To date, only a preliminary survey of the electrochemical response of these podands to anions in acetonitrile (MeCN) has been undertaken.[6]

In this study, a wide range of techniques and solvents have been employed to fully explore the electrochemistry of 1,3,5-tris(3-((ferrocenylmethyl)amino)pyridiniumyl)-2,4,6-triethylbenzene hexafluorophosphate (see structure **1**, which is now referred to as $[PD][PF_6]_3$ for convenience) from both a fundamental perspective as well as to assess anion sensing capabilities. Initially, a fundamental study of the solution-phase electrochemistry of $[PD][PF_6]_3$ was undertaken in the organic solvent,

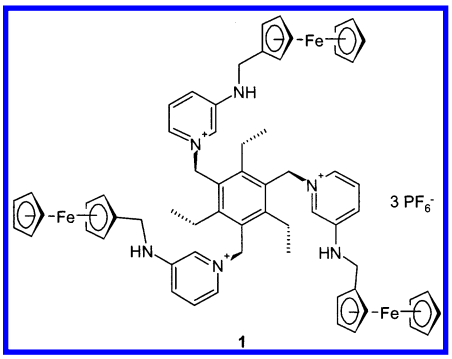

1

MeCN, containing Bu_4NPF_6 as the electrolyte. Recently, room-temperature ionic liquids have been suggested as useful alternative solvent media to organic solvents.[15−17] Of particular interest in electrochemical studies is the feature that the ionic liquid also acts as the electrolyte. Consequently, the electrochemistry of $[PD][PF_6]_3$ dissolved in the ionic liquids (1-butyl-3-methylimidazolium hexafluorophosphate (BMIM·PF_6),[18] (1-ethyl-3-methylimidazoliumyl)bis(trifluoromethylsulfonyl)amide (emim·tfsa),[16b] and (*N*-butylmethylpyrrolidiniumyl)bis(trifluoromethylsulfonyl)amide (P14·tfsa)),[19] also has been studied and data have been compared with that obtained in MeCN (0.1 M Bu_4NPF_6).

* Corresponding authors. E-mail addresses: alan.bond@sci.monash.edu.au; jon.steed@kcl.ac.uk.

10.1021/jp027699a CCC: $25.00
Published on Web 05/24/2003

Interestingly, the rate of dissolution of $[PD][PF_6]_3$ in ionic liquids, like that of ferrocene[20] is very slow. Consequently, the electrochemistry of solid $[PD][PF_6]_3$ microparticles adhered to an electrode surface[21] in contact with ionic liquids can be studied and data obtained in this manner may then be compared to the case when the compound is dissolved in the ionic liquid. Conveniently, the solid-state voltammetry of an electrode modified with water insoluble $[PD][PF_6]_3$, when it is placed in contact with aqueous media, can be studied to assess the electrochemical anion sensing capabilities of the modular podand. Significantly, $[PD][PF_6]_3$ is thermodynamically insoluble in water, so that the nature of the data obtained differs considerably from that obtained in the ionic liquid case.

In summary, the net effect of this extensive study of the electrochemistry of $[PD][PF_6]_3$ in aqueous and conventional organic solvents and ionic liquids, both dissolved and solid-state forms, is that the influence of solvent (electrolyte) and phase on the voltammetry of this ferrocene derivative is now understood in considerable detail.

Experimental Section

Chemicals. $[PD][PF_6]_3$ was synthesized, purified, and characterized by elemental analysis and ^1H NMR, as described previously.[6]

Cobaltocenium hexafluorophosphate ($[Co(Cp)_2][PF_6]$ (98%)) was purchased from Strem Chemicals. MeCN (Analytical grade) was purchased from BDH and dried overnight with basic alumina prior to use. Bu_4NPF_6 was obtained from GFS and recrystallized twice.[22] The electrolyte KPF_6 (98%) and KBF_4 were used as received from Sigma-Aldrich. KCl, NaCl, KNO_3, $NaClO_4$, $HClO_4$, Na_2HPO_4, $(NH_4)_2SO_4$, and KBr were also used as received from BDH and were of at least analytical grade purity. BMIM·PF_6 (>97%) was purchased from Sigma-Aldrich and dried over basic alumina for at least 12 h before using. Both emim.tfsa and P14·tfsa were synthesized and purified according to literature procedures.[16b,19]

Instrumentation and Procedures. Cyclic voltammetric, potential step chronoamperometric, and uncompensated resistance measurements were performed using a BAS 100B electrochemical workstation (Bioanalytical Systems). A conventional three-electrode cell was employed, with 1 mm diameter glassy carbon (GC) electrode, a 25 or a 2 μm diameter Pt microdisk electrode as the working electrode, and a Pt wire as the counter electrode. The working electrodes were polished with a 0.3 and then a 0.05 μm Al_2O_3 (Buehler) slurry, washed successively with water and acetone, and finally dried with tissue paper. The microdisk electrode radius was calibrated from the one-electron reduction of 2 mM $[Fe(CN)_6]^{3-}$ in aqueous 0.1 M KCl under near steady-state conditions using the known diffusion coefficient[23] and eq 1 (see later). For the measurements in aqueous media, an Ag/AgCl (3 M KCl) electrode was used to provide the reference potential scale. For measurements in either MeCN or ionic liquids, an Ag wire electrode was used as a quasi-reference electrode (the potential was then calibrated against that of the $[Co(Cp)_2]^{+/0}$ process in the same solution as the internal ref 24).

To prepare the ionic liquid solutions, the solvent containing solid $[PD][PF_6]_3$ was left in an ultrasonic cleaner (Unisonics Pty Ltd.). Typically, up to 2 h of sonication was required to achieve mM concentrations of $[PD][PF_6]_3$ in an ionic liquid (longest time required for BMIM·PF_6).

The procedure used for mechanical attachment of microcrystalline podand particles onto the electrode surface has been described in detail elsewhere.[25] In brief, a few milligrams of $[PD][PF_6]_3$ was placed on weighing paper. The electrode was then pressed onto and rubbed over the solid $[PD][PF_6]_3$ so that some of the microcrystalline material adhered to the electrode surface. A chemically modified electrode consisting of an array of a layer of $[PD][PF_6]_3$ microparticles adhered to the electrode surface was freshly made in this manner just prior to each voltammetric measurement.

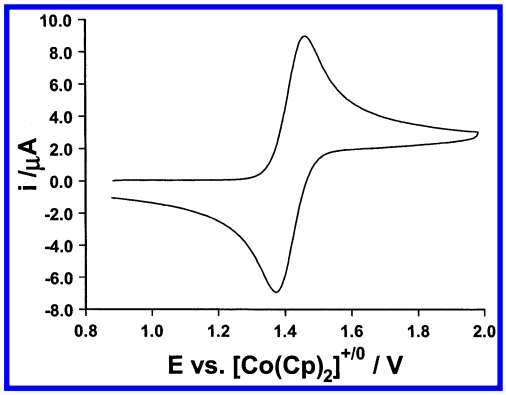

Figure 1. Cyclic voltammogram obtained for 1.2 mM $[PD][PF_6]_3$ in MeCN (0.1 M BuN_4PF_6) using a 1 mm diameter GC electrode. Scan rate = 0.2 V s^{-1}.

All electrochemical experiments were conducted at ambient temperature (20 ± 1 °C) and solutions were degassed with high-purity nitrogen for 5 min to remove oxygen, prior to undertaking electrochemical measurements. To avoid introducing water into the ionic liquids, nitrogen was passed through molecular sieves prior to being bubbled through the ionic liquid solution.

Scanning electron microscopy (SEM)-energy-dispersive X-ray (EDX) measurements on microparticles of podand on a 3 mm diameter glassy carbon electrode surface were performed using a Leica 360 field emission scanning electron microscope. The secondary electron imaging mode was used to locate the position of the sample, and the elemental composition of the sample was determined using the Oxford Link EDX system. After removal from electrolyte solution, the chemically modified electrode was carefully rinsed with distilled water to ensure the absence of adventitious ions and then dried with nitrogen prior to SEM-EDX measurements.

Results and Discussion

Solution-Phase Voltammetry of PD^{3+} in MeCN. The voltammetry of PD^{3+} dissolved in MeCN at a 1 mm diameter GC working electrode was obtained in the presence of 0.1 M Bu_4NPF_6 as the supporting electrolyte. The initial oxidation process, which is of interest in this study, is very well defined under conditions of cyclic voltammetry (Figure 1) and is associated with the ferrocene component of PD^{3+} (see structure **1**). In particular, the peak heights for the oxidation and reduction components ($I_p^{ox.}$ and $I_p^{red.}$, respectively) are equal in magnitude as required for a chemically reversible process. Furthermore, I_p^{ox} is proportional to the square root of the scan rate (υ) over the range 0.02−2 V s^{-1}, which implies that the process is diffusion-controlled. Finally, the fact that the average of the oxidation and reduction peak potentials $((E_p^{ox.} + E_p^{red.})/2)$ is constant at 1.416 ± 0.005 V vs $[Co(Cp)_2]^{+/0}$ over the same scan rate range, confirms that the process is reversible.[26]

Because PD^{3+} contains three ferrocene centers (structure 1), theoretically the initial oxidation process could be the result of an overall one-, two-, or three-electron-transfer process. The peak-to-peak potential separation (ΔE_p value) of 76 mV observed for a podand concentration of 1.2 mM at a scan rate

of 0.2 V s^{-1} is comparable to that for the well-known reversible one-electron $Fc^{0/+}$ system[22] (Fc = ferrocene) when the uncompensated solution resistance (900 Ω) effects are considered, as shown by comparison of experimental and simulated voltammograms obtained from the Digisim software package[27] (Bioanalytical Systems, West Lafayette, IN). These results imply that the PD^{3+} oxidation process also may correspond to a reversible one-electron process. However, the peak current per unit concentration of the PD^{3+} is significantly larger than that for the oxidation of ferrocene.

On the basis of assignment as a diffusion-controlled reversible one-electron-transfer process, an apparent diffusion coefficient (D) of 6.2×10^{-5} cm^2 s^{-1} would be calculated from use of the Randles−Sevcik equation[23] (ignoring the effect of any uncompensated resistance). However, such a value for PD^{3+} would be unexpectedly high, given that the diffusion coefficient of Fc is only 2.4×10^{-5} cm^2 s^{-1} in the same solvent,[28] noting that the size of PD^{3+} is significantly larger than that of Fc (according to the Stokes−Einstein equation,[29] the diffusion coefficient of a species should be inversely proportional to its radius.). Examination of the structure of the PD^{3+} cation (structure **1**), suggests that it may contain three noninteracting ferrocenyl redox centers, each of which could be oxidized by one electron at a very similar potential. Theory derived by Anson and coworkers[30] predicts that under these circumstances the voltammetric characteristics of a reversible multiple electron-transfer process may be almost indistinguishable from the reversible one-electron-transfer case, apart from the current magnitude.

To establish if a multielectron process exists for the oxidation of PD^{3+}, both near steady-state voltammetric and potential step chronoamperometric data were obtained for this diffusion-controlled reversible electron-transfer process using the same 25 μm diameter Pt microdisk electrode in both experiments.

The magnitude of the diffusion-controlled limiting current, i_d, obtained at a microdisk electrode under steady-state (slow scan rate conditions) is given by[23]

$$i_d = 4n_{total}FDac \qquad (1)$$

where n_{total} is the total number of electron transferred, F is Faraday's constant, D and c are the diffusion coefficient and concentration of PD^{3+}, respectively, and a is the radius of the electrode.

The time-dependent current, i, for a diffusion-controlled multiple electron-transfer process, recorded by potential step chronoamperometric measurements after the electrode potential is stepped from a value where there is no Faradaic process to one where the electron-transfer processes is diffusion-controlled, is governed by the relationship[23,31]

$$i_{norm} = \frac{i}{i_d} = 0.7854 + 0.8862\tau^{-1/2} + 0.2146e^{-0.7823\tau^{-1/2}} \qquad (2)$$

where $i_{norm} = i/i_d$ and $\tau = 4Dt/a^2$ are the dimensionless current and time, respectively. Equation 2 was initially derived by numerical simulation based on a one-electron transfer reaction. However, it is equally applicable to a multistep diffusion-controlled reversible electron-transfer process[23] because all electrode reactions are fast and the concentration of any intermediate is effectively zero when the potential is stepped to a sufficiently positive value. Thus, under this condition, the dimensionless transient current (eq 2) is governed solely by the diffusion of PD^{3+} so that the value of D can be obtained without knowing n_{total} or indeed even knowing the concentration of PD^{3+}. Once the value of D is known, n_{total} is then obtained via measurement of the steady-state i_d value and use of eq 1.

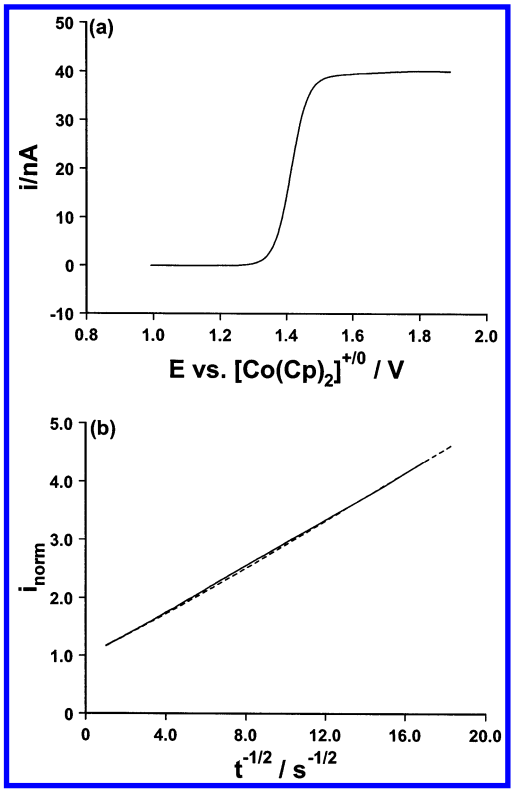

Figure 2. Electrochemical studies on the oxidation of 4.0 mM PD^{3+} in MeCN (0.20 M Bu_4NPF_6) using a 25 μm diameter Pt microdisk electrode. (a) Near steady-state voltammetry. Scan rate = 10 mV s^{-1}. (b) Chronoamperometry with a potential step from 1.25 to 1.6 V vs $[Co(Cp)_2]^{+/0}$.

Typical data obtained from near steady-state voltammetric and chronoamperometric measurements are shown in Figure 2a,b, respectively. To minimize complications arising from background (charging) current, a relatively high concentration of PD^{3+} (4.0 mM) was used. Use of data deduced from these experiments and eqs 1 and 2, led to values for the diffusion coefficient of $(7.0 \pm 0.5) \times 10^{-6}$ cm^2 s^{-1} and n_{total} of 3.0 ± 0.2 being obtained. Sensibly, the diffusion coefficient on this basis is now smaller than that of Fc and leads to the conclusion that the overall process corresponds to the reaction

$$PD^{3+}(solution) \leftrightarrows PD^{6+}(solution) + 3e^- \qquad (3)$$

That is, there appears to be minimal electronic communication between the ferrocene redox centers in the PD^{3+} cation.[30]

The difference in the quartile ($E_{1/4}$) and three quartile ($E_{3/4}$) potentials or ($E_{3/4} - E_{1/4}$) value of 57 mV obtained from the sigmoidal shaped near steady-state microdisk voltammogram shown in Figure 2a is close to the theoretical value of 55.5 mV predicted for a reversible one electron-transfer process,[26] even through data presented above confirm that it consists of three closely spaced electron-transfer processes.[30] This result is consistent with all three electron-transfer processes being reversible, but with the three ferrocene centers being noninteracting.[30]

Additional oxidation and reduction processes, presumably ligand based, also are detected (Figure 3) in the cyclic voltammetry of $[PD][PF_6]_3$ in MeCN. However, they are all significantly complicated by electrode surface interaction, as evidenced by the blocking effect the product of the second oxidation process has on the initial oxidation process (Figure

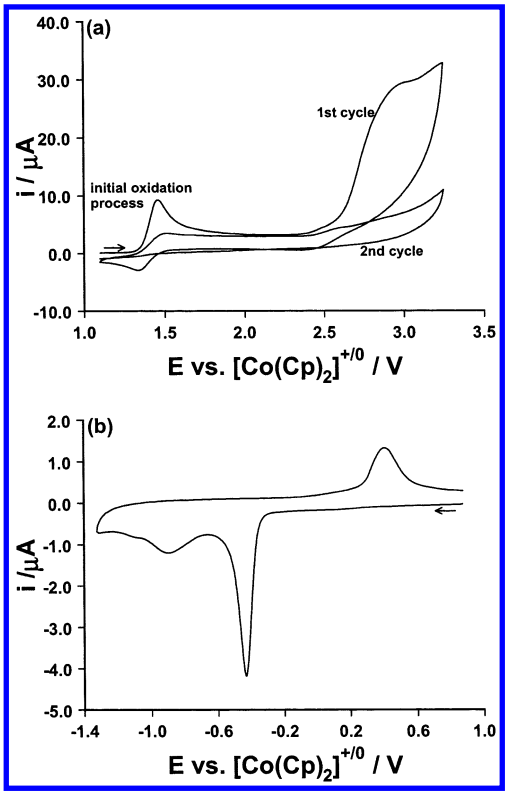

Figure 3. Cyclic voltammograms obtained at a 1 mm diameter GC electrode over wide potential range for the (a) oxidation and (b) reduction of 1.2 mM PD^{3+} in MeCN (0.1 M Bu_4NPF_6). Scan rate = 0.2 V s^{-1}.

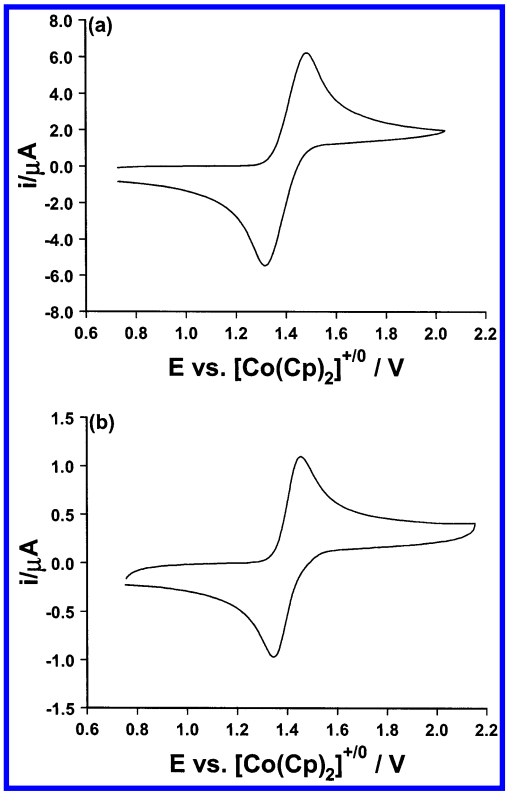

Figure 4. Comparison of cyclic voltammograms obtained at a scan rate of 0.2 V s^{-1} for oxidation of $[PD][PF_6]_3$ in BMIM·PF_6 at a GC electrode by (a) the adhered solid method and (b) the solution-phase method with 4.0 mM $[PD][PF_6]_3$.

TABLE 1: Comparison of Voltammetric Data Obtained for the PD^{3+}(solution) ⇆ PD^{6+}(solution) + $3e^-$ Oxidation Process (Equation 3) in MeCN (0.1 M Bu_4NPF_6) and in Ionic Liquids[a]

solvent	$E_{1/2}$ (V)[a] vs $[Co(Cp)_2]^{+/0}$	ΔE_p (mV)[a]	i_p^{ox} (μA)[a]	solvent viscosity (cP)	D (10^{-7} cm^2 s^{-1})[f]
MeCN	1.416 ± 0.002	73	7.49	0.33[b]	70 ± 5
BMIM·PF_6	1.401 ± 0.002	75	0.275	312[c]	0.10 ± 0.01
emim·tfsa	1.403 ± 0.002	70	0.867	35[d]	0.98 ± 0.06
P14·tfsa	1.402 ± 0.002	71	0.438	85[e]	0.25 ± 0.02

[a] Data obtained by cyclic voltammetry at a 1 mm diameter GC electrode, using a scan rate of 0.2 V s^{-1} and a 1 mM PD^{3+} concentration. [b] Measured at 30 °C.[22] [c] Measured at 30 °C.[32] [d] Measured at 20 °C.[16b] [e] Measured at 25 °C.[19] [f] Obtained from the limiting current value of a near steady-state voltammogram (25 or 2 μm diameter Pt microdisk electrode) and use of eq 1.

3a) and the symmetrical (surface confined) shape of the reduction processes (Figure 3b). In view of their complex nature, these additional processes are not discussed in any more detail.

Electrochemistry of $[PD][PF_6]_3$ Dissolved in Ionic Liquids. The cyclic voltammetry (process in eq 3) of $[PD][PF_6]_3$ dissolved in the BMIM·PF_6, emim·tfsa and P14·tfsa ionic liquids was similar to that obtained in MeCN with respect to wave shape, reversible potential vs $[Co(Cp)_2]^{+/0}$, and dependence of peak height on the scan rate. However, because of the high viscosity of the ionic liquids, the macrodisc peak current and microdisk steady-state limiting current values per unit concentration and consequently the diffusion coefficients (see eq 1 for steady-state case) are very much smaller (Table 1).

Electrochemistry of Solid $[PD][PF_6]_3$ Adhered to an Electrode Surface in Contact with Ionic Liquids. Even though the solubility of $[PD][PF_6]_3$ in the ionic liquids of interest is reasonably high, the kinetics of dissolution processes are so slow that prolonged sonication is needed to obtain millimolar concentrations (see Experimental Section). Consequently, electrochemical measurements on solid-state $[PD][PF_6]_3$ adhered to an electrode surface in contact with ionic liquids can be obtained on the voltammetric time scale without any apparent complication from $[PD][PF_6]_3$ dissolution.

Cyclic voltammograms obtained for oxidation of $[PD][PF_6]_3$ in BMIM·PF_6 under both solution-phase and adhered solid conditions are compared in Figure 4. As was the case with oxidation of Fc in this ionic liquid,[20] the voltammetric features (wave shapes, scan rate dependence of $I_p^{ox.}$, and reversible potentials) obtained from adhered solid or dissolved material are essentially indistinguishable, after allowance for slightly different levels of distortion arising from uncompensated resistance. That is, despite the fact that the magnitude of the peak current obtained by the solid-state method is significantly larger, it remains proportional to the square root of the scan rate, as expected for a diffusion-controlled process. Additional processes involving surface interaction (analogous to those shown in Figure 3) also were observed in voltammograms of both dissolved and adhered $[PD][PF_6]_3$ solid particles in BMIM·PF_6. Entirely analogous results are obtained when emim.tfsa and P14·tfsa are used instead of BMIM·PF_6.

The fact that the same reversible potential data are obtained for the first oxidation process when either adhered solid $[PD][PF_6]_3$ or dissolved PD^{3+} are employed can be rationalized if it is assumed that at least one of the solid-state oxidized forms of PD^{3+} (PD^{4+}, PD^{5+}, or PD^{6+}) dissolves in the ionic liquid and remains dissolved during the remaining part of the cyclic voltammetric experiment[20] (thermodynamically soluble oxidized form and slow reprecipitation kinetics). An example of a possible overall process for the oxidation of adhered $[PD][PF_6]_3$-(solid) under these circumstances is given in the reaction

sequence described by eqs 4a−c and which could take place at the pod and microparticles/electrolyte solution interface.

$$[PD][PF_6]_3(\text{solid}) + 3PF_6^-(\text{ionic liquid}) \leftrightarrows [PD][PF_6]_6(\text{solid}) + 3e^- \quad (4a)$$

$$[PD][PF_6]_6(\text{solid}) \rightleftarrows PD^{6+}(\text{ionic liquid}) + 6PF_6^-(\text{ionic liquid}) \quad (4b)$$

$$PD^{6+}(\text{ionic liquid}) + 3e^- \leftrightarrows PD^{3+}(\text{ionic liquid}) \quad (4c)$$

Solid-State Electrochemistry of a $[PD][PF_6]_3$ Modified Electrode in Contact with Aqueous Electrolyte Media. In contrast to the situation prevailing in ionic liquids, $[PD][PF_6]_3$ is thermodynamically insoluble in water. If the oxidized forms of $[PD][PF_6]_3$ also are thermodynamically insoluble in water, then when a $[PD][PF_6]_3$ modified electrode is in contact with an aqueous electrolyte containing anion (A^-), the reaction sequence given in eqs 5−7 should be dominant at the podand microparticles/electrolyte solution interface, rather than a reaction scheme of the kind given in eq 4 that is believed to apply in ionic liquids.

$$[PD^{3+}][PF_6]_{3-n}[A]_n(\text{solid}) + A^-(\text{aqueous}) \leftrightarrows [PD^{4+}][PF_6]_{3-n}[A]_{n+1}(\text{solid}) + e^- \quad (5)$$

$$[PD^{4+}][PF_6]_{3-n}[A]_{n+1}(\text{solid}) + A^-(\text{aqueous}) \leftrightarrows [PD^{5+}][PF_6]_{3-n}[A]_{n+2}(\text{solid}) + e^- \quad (6)$$

$$[PD^{5+}][PF_6]_{3-n}[A]_{n+2}(\text{solid}) + A^-(\text{aqueous}) \leftrightarrows [PD^{6+}][PF_6]_{3-n}[A]_{n+3}(\text{solid}) + e^- \quad (7)$$

That is, interconversion of solids in different redox levels may take place by a rate-determining nucleation/growth process on the voltammetric time scale. However, irrespective of the details of the mechanism, to maintain charge neutrality, the oxidation of solid $[PD][PF_6]_3$ adhered to an electrode surface requires that the electrolyte anion A^- transfers from solution phase to solid phase. Furthermore, the reduction component of this kind of cyclic voltammetric experiment requires that either A^- or PF_6^- contained in the solid phase be transported into the solution phase. Equations 5−7 also include the possibility that an $A^- \leftrightarrows PF_6^-$ ion exchange process will occur, as is likely under conditions where a high concentration of aqueous electrolyte anion A^- is present. Under these solid-state conditions, selectivity of $[PD][PF_6]_3$ for particular electrolyte anions is possible, at least in principle, if either the rate or the free energy of the nucleation/growth process associated with the solid−solid transformation is significantly anion dependent.

If any of the electron oxidation products are sparingly soluble and the dissolution kinetics are rapid, there may exist an equilibrium between the solution and solid-state forms that is governed by the solubility product. Moreover, if the solubilities of podand in different redox states vary, significant levels of both dissolution and reprecipitation reactions could accompany the cyclic voltammetry of adhered solid $[PD][PF_6]_3$. In this case, the dependence of the $[PD][PF_6]_3$(solid) voltammetry on the electrolyte anion could depend on the solubility products as well as the details of the nucleation/growth processes.

To probe some of the details of the mechanisms that apply to the electrochemical oxidation of solid $[PD][PF_6]_3$ adhered to an electrode in contact with aqueous electrolyte media, and also

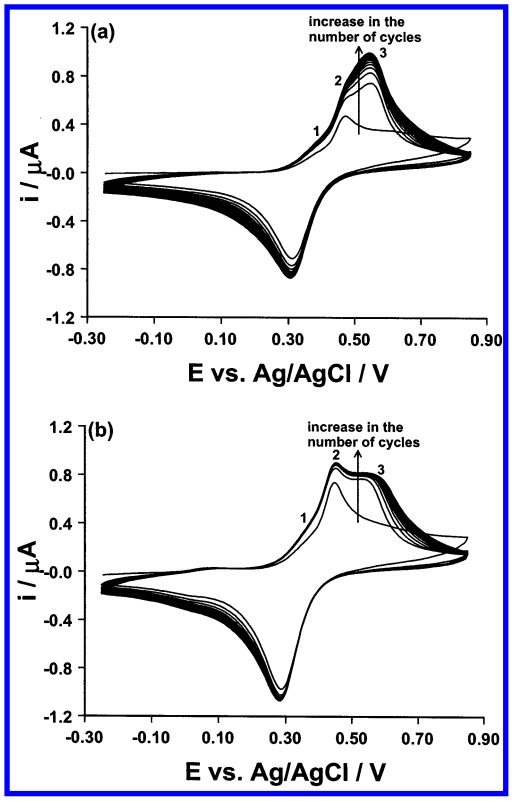

Figure 5. Influence of the aqueous KPF_6 electrolyte concentration (a) 0.1 M and (b) 0.4 M on the cyclic voltammetry (20 cycles) of solid $[PD][PF_6]_3$ adhered to a 1 mm diameter GC electrode. Scan rate = 0.1 V s^{-1}.

whether this process can be used as an electrochemical anion sensor,[6b] the effect of the electrolyte anions and their aqueous solution concentration was examined. The electrolytes chosen for this study were KPF_6, $NaClO_4$, $HClO_4$, KCl, NaCl, KBr, KNO_3, $(NH_4)_2SO_4$, Na_2HPO_4, and KBF_4.

The solid-state voltammograms of $[PD][PF_6]_3$ microparticles mechanically adhered to a glassy carbon electrode placed in contact with aqueous solutions containing different concentrations of KPF_6 represents the simplest case where the PF_6^- anion is common to the solid and electrolyte phases. As shown in Figure 5, where the first twenty cycles of the potential are displayed, the shape of the cyclic voltammogram obtained in the first cycle is markedly different from that detected in subsequent cycles and also different from that observed in ionic liquids. Furthermore, unlike the case with ionic liquids, wave splitting is detected on the oxidation component of the cyclic voltammogram. Particularly noteworthy is the fact that in second and subsequent cycles, three well-resolved oxidation peaks are detected, which implies that the oxidation components of the three one-electron transfer processes are now resolved. Under the conditions of Figure 5a, on repetitive cycling of the potential, the peak height increases slightly in cycles 2−10, then remains almost unchanged until about cycle 60, after which a very slight decrease in peak height occurs.

Examination of voltammograms in Figure 5 also shows that when the concentration of PF_6^-(aqueous) is increased from 0.1 to 0.4 M, the peak height for the oxidation process 3 becomes significantly diminished. In the presence of 0.4 M PF_6^- electrolyte, the peak height increases slightly in the first 5 cycles, then remains essentially unchanged for 80 cycles of the potential. These experiments conducted over extended periods of time imply that dissolution of solid is minimal when the electrolyte anion is PF_6^-. The concentration dependence of the voltammetry

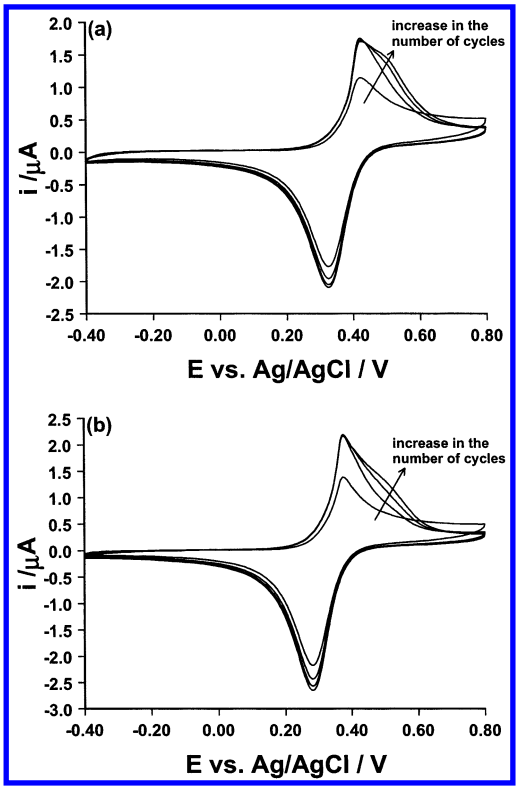

Figure 6. Influence of the aqueous $NaClO_4$ electrolyte concentration (a) 0.1 and (b) 1.0 M on the cyclic voltammetry of solid $[PD][PF_6]_3$ adhered to a 1 mm diameter GC electrode. Scan rate = 0.1 V s^{-1}.

may be due to a decrease in solubility of the three-electron oxidized $[PD][PF_6]_6$ species associated with the enhanced concentration of PF_6^-(aqueous) or else to a change in rate of the nucleation/growth processes. Resolution in the oxidation waves of the cyclic voltammogram also may be due to the different rate or free energy of ingress of PF_6^- in the three oxidation steps because this process may become less favorable as more anions need to enter the solid and a single rate or free energy for anion expulsion in the reduction steps. However, because many details of the mechanism of the oxidation of solid $[PD][PF_6]_3$ microparticles adhered to an electrode surface in contact with aqueous KPF_6 electrolyte are unknown, further speculation is unwarranted.

With $NaClO_4$ as the electrolyte (Figure 6), a shoulder rather than three resolved peaks is detected after a number of cycles of the potential. When the concentration of ClO_4^- is increased from 0.1 to 1 M, the magnitude of the shoulder is suppressed, which could again be associated with the dependence of the solubility of an oxidized species on the anion concentration or rate changes in the nucleation/growth step. Data obtained with $HClO_4$ are essentially the same as with $NaClO_4$ as the electrolyte, implying that the identity of the cation is not important, as expected, if charge neutralization, via incorporation of anion into the solid state is the rate-determining step. With extensive cycling of the potential, the peak current magnitude starts to decrease, which is consistent with very slow dissolution of oxidized solid.

NMR data[6b] obtained when the $[PD][PF_6]_3$ is dissolved in MeCN suggest that the podand may be used as a Cl^- sensor because the Cl^- binding constant is far larger than for other anions. To establish whether the solid-state voltammogram of $[PD][PF_6]_3$ exhibits chloride specific sensing characteristics, the effect of aqueous chloride electrolyte was examined. Voltammograms shown in Figure 7 reveal in this case that the peak current increases with Cl^- concentration, and the shapes are

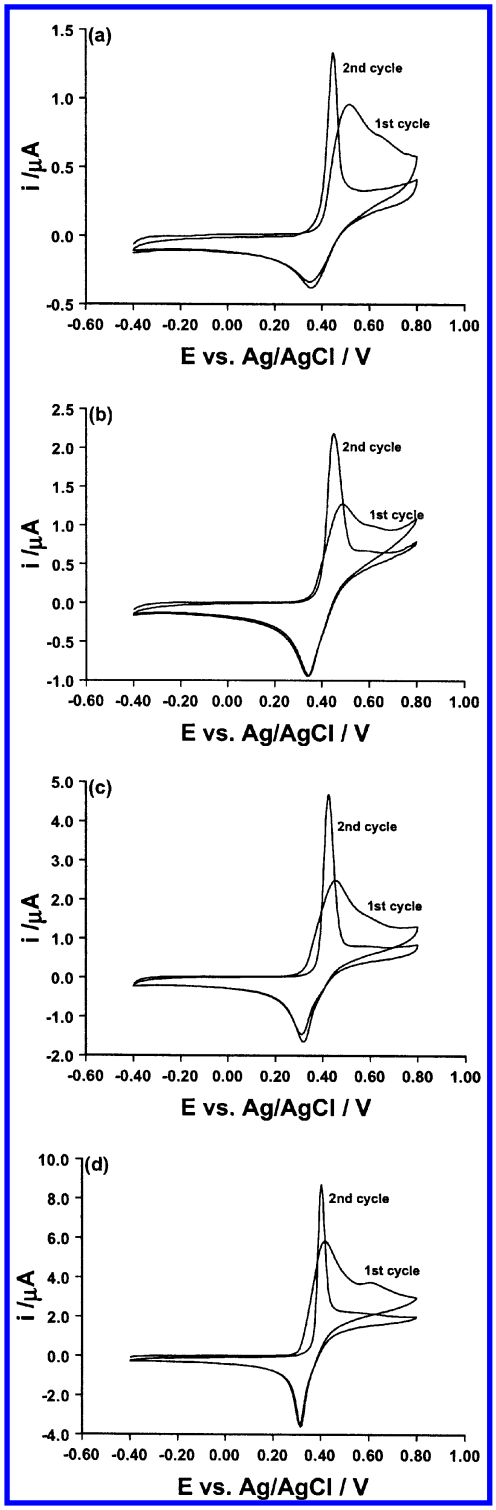

Figure 7. Effect of the Cl^- concentration (a) 0.01, (b) 0.05, (c) 0.1, and (d) 1 M NaCl on the voltammetry of solid $[PD][PF_6]_3$ adhered to a 1 mm diameter GC electrode. Scan rate = 0.1 V s^{-1}.

distinctly different from those in Figures 5 (PF_6^-) and 6 (ClO_4^-), with no evidence of resolved oxidation processes being detected on second and subsequent cycles of the potential. When chloride is the electrolyte, the voltammograms change shape from one with mass transport apparently governed by semi-infinite diffusion in the first voltammetric cycle (as is the case in an ionic liquid) to one exhibiting the characteristics of a stripping voltammogram[23,33] in the second and subsequent cycles of the potential. However, the peak potential shifts to slightly less positive potentials with increasing chloride concentration, which

is consistent with the situation prevailing when either KPF_6 or $NaClO_4$ is the supporting electrolyte.

Noteworthy observations accompanying the cyclic voltammogram with KCl as the electrolyte include the following: (a) The area (charge) associated with the oxidation process in the first cycle is very large relative to the second and subsequent cycles. (b) Peak widths at half-height are much smaller than expected for a diffusion-controlled process. (c) A steady-state current was observed at potentials more positive than 0.5 V vs Ag/AgCl in the second and subsequent cycles. (d) On extended cycling of the potential, the peak height starts to diminish. (e) Replacement of KCl with NaCl as the electrolyte does not significantly influence the voltammetry. All these features suggest that oxidation of arrays of microparticles of $[PD][PF_6]_3$(solid) leads initially (eq 8) to ion exchange to produce $[PD][Cl]_6$(solid), which in the initial stage of oxidation forms water

$$[PD][PF_6]_3(\text{solid}) + 6Cl^-(\text{aqueous}) \leftrightharpoons [PD][Cl]_6(\text{solid}) + 3PF_6^-(\text{aqueous}) + 3e^- \quad (8)$$

soluble PD^{6+}, as in eq 9, although of course the solubility arises at the PD^{4+} or PD^{5+} states of the overall three-electron process.

$$[PD][Cl]_6(\text{solid}) \leftrightharpoons PD^{6+}(\text{aqueous}) + 6Cl^-(\text{aqueous}) \quad (9)$$

On the reverse potential or reduction scan, PD^{6+}(aqueous) is reduced back to PD^{3+}(aqueous) (see eq 10), some of which reprecipitated on the bare part of the electrode surface to give a thin film, as in eq 11.

$$PD^{6+}(\text{aqueous}) + 3e^- \leftrightharpoons PD^{3+}(\text{aqueous}) \quad (10)$$

$$PD^{3+}(\text{aqueous}) + 3Cl^- \leftrightharpoons [PD][Cl]_3(\text{thin film}) \quad (11)$$

In the oxidation component of the second cycle of the potential, the thin film is stripped from the electrode surface to generate PD^{6+}(aqueous) as in

$$[PD][Cl]_3\ (\text{thin film}) + 3\ Cl^-\ (\text{aqueous}) \rightleftharpoons [PD][Cl]_6\ (\text{thin film}) + 3\ e^-$$
$$\Updownarrow$$
$$PD^{6+}\ (\text{aqueous}) + 6\ Cl^-\ (\text{aqueous}) \quad (12)$$

The reaction scheme differs from that in the ionic liquid, because in the latter case, both halves of the redox couple (PD^{3+} and PD^{6+}) are thermodynamically soluble. Consequently, no reprecipitation can occur when PD^{6+}(ionic liquid) is reduced back to PD^{3+}(ionic liquid). The mechanism proposed explains the following observations: the smaller oxidative charge associated with the second cycle is a result of loss of PD^{6+}(aqueous) or PD^{3+}(aqueous) into bulk solution by diffusion; the wave shape difference on the first and second cycles is a consequence of transformation of arrays of microparticles of $[PD][PF_6]_3$(solid) to $[PD][Cl]_3$(thin film); the steady-state current at positive potentials in second and subsequent cycles is a result of oxidation of PD^{3+}(aqueous) or PD^{4+}(aqueous) to PD^{6+}(aqueous) at pinholes[34,35] formed when microparticle dissolution and loss of initially present $[PD][PF_6]_3$(solid) (or $[PD][Cl]_3$)(solid) occurs in the oxidation/dissolution $\leftrightharpoons$ reduction/reprecipitation sequence; the difference of voltammograms observed when either PF_6^- or ClO_4^- are electrolyte anions is related to the relatively insoluble nature of oxidized $[PD][PF_6]_6$ and $[PD][ClO_4]_6$ compared to $[PD][Cl]_6$ (or to a less oxidized intermediate).

Voltammograms obtained in the presence of Br^-, NO_3^-, SO_4^{2-}, HPO_4^{2-}, and BF_4^- anions (KBr, KNO_3, $(NH_4)_2SO_4$, Na_2HPO_4, and KBF_4 electrolyte, respectively) are analogous to those obtained in the presence of Cl^-. Importantly, peak potentials, peak currents, and the shapes of the voltammograms are not highly dependent on the identity of these electrolyte anions (Table 2) unlike the situation that could be expected for a fully solid-state process.[36] However, the average values of the peak potentials ($(E_p^{ox.} + E_p^{red.})/2$) for the $PD^{3+/6+}$ process is approximately 1.5 V vs $[Co(Cp)_2]^{+/0}$ in aqueous media, which is in the same potential region as the reversible potentials obtained in MeCN and ionic liquids. (This value is calculated by noting that the standard potential of Ag/AgCl (3 M KCl) and Fc/Fc^+ in aqueous electrolyte media are 0.212[37] and 0.44[22] vs NHE, respectively, and that the formal potential of Fc/Fc^+ is 1.35 V vs $[Co(Cp)_2]^{+/0}$ in a wide range of solvents.[24])

TABLE 2: Dependence of Electrolyte Anion on the Cyclic Voltammetric Data Obtained When $[PD][PF_6]_3$ Adhered to a 1 mm Diameter Glassy Carbon Electrode[a] Is in Contact with 0.1 M Concentration of Aqueous Electrolyte

	$E_p^{red.}$ (V vs Ag/AgCl)		$E_p^{ox.}$ (V vs Ag/AgCl)		
supporting electrolyte	first cycle	second cycle	first cycle	second cycle	$\Delta E_{p,1/2}$[b]
KBr	0.331	0.339	0.444	0.462	0.095
KNO_3	0.345	0.347	0.432	0.459	0.096
$(NH_4)_2SO_4$	0.311	0.322	0.473	0.434	0.076
Na_2HPO_4	0.336	0.324	0.500	0.443	0.049
KBF_4	0.373	0.375	0.439	0.471	0.095

[a] Scan rate is 0.1 V s^{-1}. [b] Width at half-height of stripping peak observed in the second cycle of the potential.

The decrease in peak current observed in the third and subsequent cycles of potential when any of the above-mentioned salts are present as the supporting electrolyte is very significant when a slow scan rate of 0.02 V s^{-1} is employed, and much larger than found at higher scan rates (0.1−1.0 V/s) and also significantly larger than found in the presence of either PF_6^- or ClO_4^- electrolyte anions. This result is again consistent with the dissolution component of the mechanism being less significant when PF_6^- or ClO_4^- are used as the electrolyte anions.

If solubility is a major factor, then voltammetry in mixed electrolyte media should be dominated by that encountered with the electrolyte anion that allows the smallest level of dissolution. Cyclic voltammograms with solid $[PD][PF_6]_3$ adhered to a glassy carbon electrode therefore were examined in the presence of mixed aqueous electrolytes. Experiments in mixed Cl^- and PF_6^- electrolyte media showed that even with a $[Cl^-]$:$[PF_6^-]$ ratio of 20:1 (total concentration 1.05 M), the voltammogram still exhibited most of the characteristics detailed above for pure 0.1 M PF_6^- electrolyte.

To confirm that PF_6^- is preferentially incorporated into the microcrystalline lattice of $[PD][PF_6]_3$, a $[PD][PF_6]_3$ chemically modified electrode was placed in contact with a mixed electrolyte solution containing a 1:1 ratio of PF_6^- and Cl^- (total concentration of 0.2 M) for 5 min without applying an external potential. The electrode was removed from the solution and rinsed with distilled water to remove any residual electrolyte and finally dried with nitrogen gas. The results of the EDX analysis of podand adhered to this electrode showed no evidence of chloride having incorporated into the solid. Furthermore, the ratio of the P and Fe EDX peaks remained the same as obtained from a $[PD][PF_6]_3$ sample that had not been in contact with the electrolyte solution. SEM-EDX measurements were also carried out on a podand-modified electrode that had been subjected to controlled potential electrolysis at 0.7 V vs Ag/AgCl in the same 1:1 mixed electrolyte solution for 5 min. This potential should lead to formation of the three-electron oxidized species. Fol-

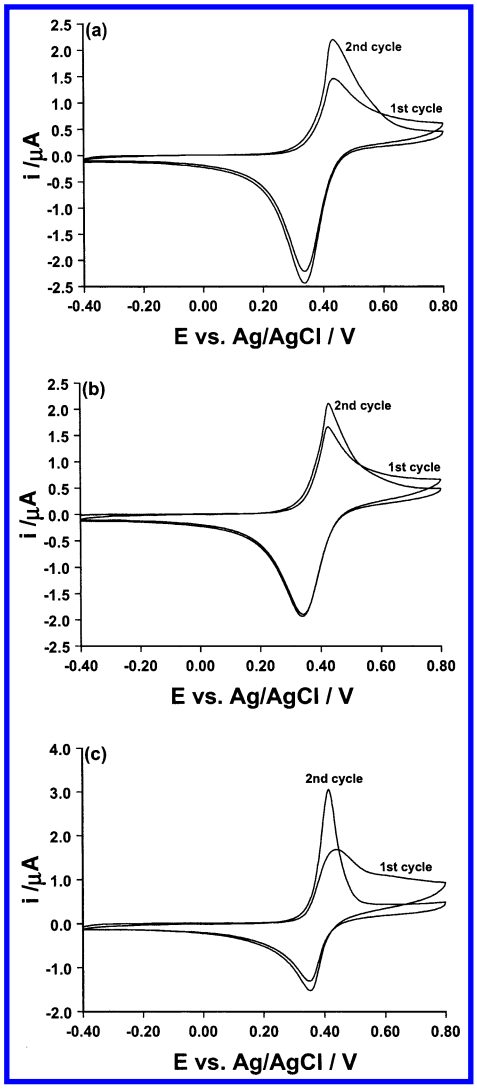

Figure 8. Voltammetry of solid-state $[PD][PF_6]_3$ in the presence of different concentration ratio of Cl^- and ClO_4^- in the solution (concentration of the less concentrated species = 0.05 M). (a) [NaCl]:[$NaClO_4$] = 1:2, (b) [NaCl]:[$NaClO_4$] = 2:1 and (c) [NaCl]:[$NaClO_4$] = 20:1.

lowing the same electrode treatment as described above, EDX data showed that the ratio of the P and Fe peaks had significantly increased, as expected if $[PD][PF_6]_3$(solid) is converted to $[PD][PF_6]_6$(solid). Importantly, no chlorine could be detected by the EDX method of elemental analysis. These data support the conclusion that PF_6^- is preferentially incorporated into the lattice of the podand in both the reduced and oxidized forms of the solid in the presence of mixed PF_6^- and Cl^- electrolyte media.

In contrast, when voltammetric investigations were carried out in mixed ClO_4^- and PF_6^- electrolyte media with a concentration ratio of 1:2 or 2:1 (total concentration of 0.10 M), the features observed were a combination of those obtained with 0.1 M single anion situation. Results shown in Figure 8 reveal that voltammograms in mixed ClO_4^-:Cl^-electrolyte media are similar to those obtained in pure aqueous ClO_4^- or PF_6^- electrolyte media, except when the concentration of Cl^- is in a very large excess. Voltammetric investigations in other mixed electrolyte media containing either PF_6^- or ClO_4^- and other electrolytes are always dominated by the "hexafluorophosphate" or "perchlorate" type response. All observations in mixed electrolyte media are again consistent with voltammetry having a relatively small dissolution component when PF_6^- or

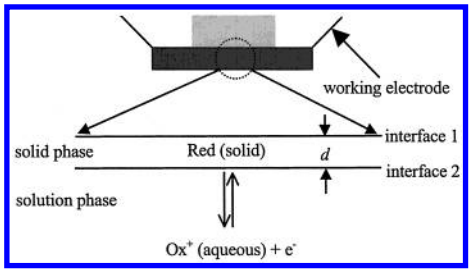

Figure 9. Schematic representation of the voltammetry of a solid adhered to an electrode in contact with aqueous electrolyte media when the oxidation product is sparingly soluble.

ClO_4^- electrolyte are present, compared to the situation prevailing with other electrolytes considered in this study.

Results obtained in mixed electrolyte media suggest that it is unlikely to be possible to use the voltammetry of $[PD][PF_6]_3$(solid) as an anion sensor on the basis of achievement of high selectivity toward a particular anion. This is different from circumstances based on NMR measurements in MeCN[6b] where the selectivity of dissolved PD^{3+}(solution) to an anion only depends on the relative magnitude of the binding constants rather than the relative behavior in both the PD^{3+} and PD^{6+} redox levels.

Theoretical Treatment of the Voltammetry of $[PD][PF_6]_3$ Microparticles Adhered to an Electrode Surface Placed in Contact with Aqueous Electrolyte Media. Transformation in voltammetric wave shape on second and subsequent cycles of the potential has been attributed to a change in particle thickness caused by a dissolution/reprecipitation process. If complications associated with ion exchange, dissolution/reprecipitation, and multielectron reactions are neglected, the total equivalent reaction can be represented by the scheme shown in Figure 9 and summarized by eq 13, which is the sum of eqs 14 and 15, where MA is the aqueous supporting electrolyte.

$$\text{total reaction:}\quad \text{Red.(solid)} \rightleftarrows \text{Ox.}^+\text{(aqueous)} + e^- \quad (13)$$

$$\text{Red.(solid)} + A^-\text{(aqueous)} \rightleftarrows \text{[Ox.][A](solid)} + e^- \quad (14)$$

$$\text{[Ox.][A](solid)} \rightleftarrows \text{Ox.}^+\text{(aqueous)} + A^-\text{(aqueous)} \quad (15)$$

Thus, in modeling the simplified reaction scheme, it is assumed that the electron-transfer process (eq 14) is reversible and that equilibrium of the "dissolution" process (eq 15) is achieved on the voltammetric time scale. Consequently, it is assumed that concentrations of the redox couple at the electrode surface are governed by the Nernst equation for the process described by eq 13. Thus, the theoretical model is analogous to ones commonly used in thin film stripping voltammetry.[23,33] According to this theoretical concept: the electron-transfer process is assumed to occur at interface 2; Red.(solid) is always surface confined; the mass transport of Ox.(solution) is governed by semi-infinite linear diffusion; the theoretical analysis does not take into account any change of film thickness that would occur during the dissolution process; the charge transport mechanism is one in which the electron and ion transport are coupled in the solid to achieve charge neutralization so that the overall diffusion problem is treated by employing a concept of an apparent diffusion coefficient.[38,39] In summary, the electron transfer and mass transport mechanisms of an ideal solid are adopted for the surface-confined species.[40] Consequently, the mole fraction of Red.(solid) present in a single phase solid is assumed to be proportional to the activity. Treatment of a film of variable thickness (d) can clearly be accommodated by this

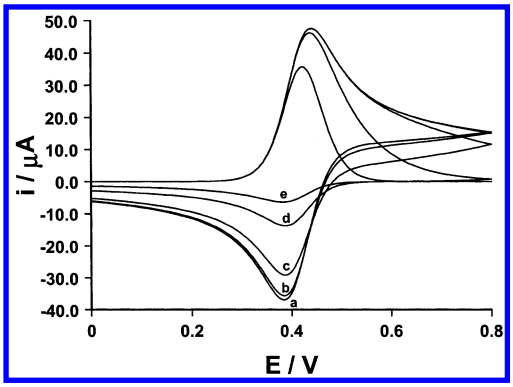

Figure 10. Influence of the film thickness, *d*, on voltammograms simulated according to the postulated mechanism. $D_{Red.} = 5 \times 10^{-9}$ cm^2 s^{-1}, $d = 5 \times 10^{-4}$ (a), 3×10^{-4} (b), 2×10^{-4} (c), 1×10^{-4} (d), and 5×10^{-5} (e) cm and the other parameters are as defined in the text.

model. The best known use of this kind of model involves amalgam stripping voltammetry.[23,33]

If a one-dimensional linear diffusion equation is applied to this model then

$$\frac{\partial c}{\partial t} = D\frac{\partial^2 c}{\partial x^2} \tag{16}$$

where *c* is the concentration of the species of interest (Red.(solid) and Ox.(solution)), *t* is time and *x* is the distance from interface 2.

The above assumptions lead to the following initial and boundary conditions:

$$t = 0, \text{ in the solid phase:} \qquad c(\text{Red.(solid)}) = c^*$$

$$t = 0, \text{ in the solution phase:} \qquad c(\text{Ox.(solution)}) = 0$$

$$t > 0, \text{ interface 2:} \qquad \frac{c(\text{Ox.(solution)})}{c(\text{Red.(solid)})} = \exp\left[\frac{F}{RT}(E - E^{0\prime})\right]$$

$$\sum D\frac{\partial c}{\partial x} = 0 \qquad \text{for the redox couple}$$

$$t > 0, \text{ interface 1 } (x = d): \qquad D_{\text{Red.}}\frac{\partial c(\text{Red.(solid)})}{\partial x} = 0$$

$$t > 0, x = \infty: \qquad c(\text{Ox.(solution)}) = 0$$

In these relationships, *F*, *R*, and *T* have their usual meanings, $E^{0\prime}$ is the formal potential of the electrode reaction process (eq 13), and $D_{Red.}$ is the diffusion coefficient of Red.

The problem to be addressed can be cast into a dimensionless form using the same combination of parameters as used by Nicholson and Shain[41] and then solved numerically, using the Crank−Nicolson implicit finite difference method.[42] To improve both the efficiency and the accuracy of the simulation, an expanding grid originally introduced by Feldberg[43] was adopted. The theoretical results presented in this study employed the following parameters: $c^* = 1$ M, which is an arbitrary value, $E^{0\prime} = 0.5$ V, diffusion coefficient of Ox. $D_{Ox.} = 5 \times 10^{-6}$ cm^2 s^{-1}, scan rate = 0.1 V s^{-1}, radius of electrode = 0.05 cm, with other parameters being defined in the figure captions.

The simulated voltammograms in Figure 10 reveals how a voltammogram having the characteristics of a stripping voltammogram can arise if the thickness of the film decreases from 5×10^{-4} (Figure 10, curve a) to 5×10^{-5} cm (Figure 10, curve e) (diffusion within the solid changes from semi-infinite to finite diffusion). In the experimental situation, arrays of microparticles are initially present on the surface. The redistribution of the podand on the electrode surface due to the oxidation−dissolution/reduction−reprecipitation process effectively leads to a decrease of the film thickness, but with a higher overall surface coverage. Clearly the simplified model only encompasses some aspect of the voltammetry when microparticles are adhered to an electrode in contact with water, so any detailed comparison of simulated and experimental data is unwarranted.

Conclusions

The voltammetry of the dissolved modular podand PD^{3+}(solution) in MeCN and the ionic liquids, BMIM·PF_6, emim.tfsa, and P14·tfsa, exhibits an overall three-electron oxidation process consisting of three very closely spaced one-electron-transfer steps, which implies that minimal electronic communication exists between the three ferrocenyl redox active centers.[30]

Voltammograms of dissolved PD^{3+} in ionic liquids have characteristics similar to those observed in MeCN. However, because the kinetics of dissolution of solid $[PD][PF_6]_3$ in ionic liquids is slow, the electrochemistry of microparticles mechanically attached to the electrode surface in contact with the ionic liquids is obtained. Interestingly, these apparently solid-state voltammogram exhibit the same characteristics of those obtained when $[PD][PF_6]_3$ is dissolved in the ionic liquids. This result confirms that it is possible to establish the ionic liquid solution-phase voltammetric behavior of slowly dissolving compounds, in agreement with earlier studies on ferrocene and other redox processes in ionic liquids.[20]

Solid-state voltammograms of $[PD][PF_6]_3$ when the chemically modified electrode is in contact with aqueous media (electrolyte) are very different from the ionic liquid case. In this case, $[PD][PF_6]_3$ is thermodynamically insoluble in water, but the oxidized forms are believed to have a variable level of the solubility, which explains the dependence of the aqueous electrolyte anion. An oxidation−dissolution/reduction−reprecipitation and ion exchange type mechanism is consistent with the experimental observations.

Acknowledgment. King's College London (visiting fellowship award to J.W.S.), Monash University (research fellowship award to J.Z.) and the Australian Research Council are thanked for financial support of this Kings College-Monash University collaborative research program. Prof. Douglas MacFarlane and Mr. Stewart Forsyth (School of Chemistry, Monash University) are gratefully acknowledged for provision of the emim.tfsa and P14·tfsa ionic liquids.

References and Notes

(1) Antonisse, M. M. G.; Reinhoudt, D. N. *Chem. Commun.* **1998**, 443.

(2) (a) *Host−guest Molecular Interactions: from Chemistry to Biology*; Ciba Foundation Symposium 158; Wiley: Chichester, U.K., 1991. (b) Steed, J. W.; Atwood, J. L. *Supramolecular Chemistry*; Wiley: Chichester, U.K., 2000.

(3) (a) Sun, S. S.; Lees, A. J. *Coord. Chem. Rev.* **2002**, *230*, 171. (b) Gale, P. A. *Coord. Chem. Rev.* **2001**, *213*, 79. (c) Metzger, A.; Gloe, K.; Stephan, H.; Schmidtchen, F. P. *J. Org. Chem.* **1996**, *61*, 2051.

(4) Xue, G.; Savage, P. B.; Bradshaw, J. S.; Zhang, X.; Izatt, R. M. *Adv. Supermol. Biochem.* **2000**, *7*, 99.

(5) Gunnlaugsson, T.; Davis, A. P.; Glynn, M. *Chem. Commun.* **2001**, 2556.

(6) (a) Abouderbala, L. O.; Belcher, W. J.; Boutelle, M. G.; Cragg, P. J.; Dhaliwal, J.; Fabre, M.; Steed, J. W.; Turner, D. R.; Wallace, K. J. *Chem. Commun.* **2002**, 358. (b) Abouderbala, L. O.; Belcher, W. J.; Boutelle, M. G.; Cragg, P. J.; Steed, J. W.; Turner, D. R.; Wallace, K. J. *Proc. Natl. Acad. Sci. U.S.A.* **2002**, *99*, 5001.

(7) Antonisse, M. M. G.; Reinhoudt, D. N. *Electroanalysis* **1999**, *11*, 1035.

(8) Qian, Q. S.; Wilson, G. S.; Bowman-James, K.; Girault, H. H. *Anal. Chem.* **2001**, *73*, 497.
(9) Beer, P. D.; Gale, P. A. *Angew. Chem., Int. Ed.* **2001**, *40*, 487.
(10) Beer, P. D.; Cadman, J. *Coord. Chem. Rev.* **2000**, *205*, 131.
(11) (a) Beer, P. D. *Acc. Chem. Res.* **1998**, *31*, 71. (b) Staffilani, M.; Hancock, K. S. B.; Steed, J. W.; Holman, K. T.; Atwood, J. L.; Juneja, R. K.; Burkhalter, R. S. *J. Am. Chem. Soc.* **1997**, *119*, 6324. (c) Holman, K. T.; Orr, G. W.; Steed, J. W.; Atwood, J. L. *Chem. Commun.* **1998**, 2109.
(12) Mei, M.; Wu, S. *New J. Chem.* **2001**, *25*, 471.
(13) Morozumi, T.; Anada, T.; Nakamura, H. *J. Phys. Chem. B* **2001**, *105*, 2923.
(14) McSkimming, G.; Tucker, J. H. R.; Bouas-Laurent, H.; Desergne, J. P. *Angew. Chem., Int. Ed. Engl.* **2000**, *39*, 2167.
(15) (a) Sheldon, R. *Chem. Commun.* **2001**, 2399. (b) Adam, D. *Nature* **2000**, *407*, 938. (c) Welton, T. *Chem. Rev.* **1999**, *99*, 2071.
(16) (a) Kubo, W.; Kitamura, T.; Hanabusa, K.; Wada, Y.; Yanagida, S. *Chem. Commun.* **2002**, 374. (b) Bonhôte, P.; Dias, A. P.; Papageorgiou, N.; Kalyanasundaram, K.; Grätzel, M. *Inorg. Chem.* **1996**, *35*, 1168.
(17) (a) Visser, A. E.; Holbrey, J. D.; Rogers, R. D. *Chem. Commun.* **2001**, 2484. (b) Chun, S.; Dzyuba, S. V.; Bartsch, R. A. *Anal. Chem.* **2001**, *73*, 3737. (c) Visser, A. E.; Swatloski, R. P.; Reichert, W. M.; Griffin, S. T.; Rogers, R. D. *Ind. Eng. Chem. Res.* **2000**, *39*, 3596. (d) Visser, A. E.; Swatloski, R. P.; Rogers, R. D. *Green Chem.* **2000**, *2*, 1.
(18) Gordon, C. M.; McCluskey, A. *Chem. Commun.* **1999**, 1431.
(19) MacFarlane, D. R.; Meakin, P.; Sun, J.; Amini, N.; Forsyth, M. *J. Phys. Chem. B* **1999**, *103*, 4164.
(20) Zhang, J.; Bond, A. M. *Anal. Chem.* **2003**, *75*, 2694.
(21) (a) Scholz, F.; Meyer, B. In *Electroanalytical Chemistry*; Bard, A. J., Ed.; Marcel Dekker: New York, 1998; Vol. 20, p 1 (see also references therein). (b) Chlistunoff, J.; Cliffel, D.; Bard, A. J. In *Handbook of Conductive Molecules and Polymers*; Nalwa, H. S., Ed.; Wiley: Chichester, U.K., 1997; Vol. 1, Chapter 7 (see also references therein).
(22) Sawyer, D. T.; Sobkowiak, A.; Roberts, J. L., Jr. *Electrochemistry for Chemist*, 2nd ed.; Wiley: New York, 1995.
(23) Bard, A. J.; Faulkner, L. R. *Electrochemical Methods, Fundamental and Applications*, 2nd ed.; Wiley: New York, 2001; pp 168−221, 231, 471−528.
(24) Stojanovic, R. S.; Bond, A. M. *Anal. Chem.* **1993**, *65*, 56.
(25) Bond, A. M.; Cooper, J. B.; Marken, F.; Way, D. M. *J. Electroanal. Chem.* **1995**, *396*, 407.
(26) Oldham, K. B.; Myland, J. C. *Fundamental of Electrochemical Science*; Academic Press: San Diego, 1994; p 209.
(27) Rudolph, M.; Reddy, D. P.; Feldberg, S. W. *Anal. Chem.* **1994**, *66*, 589A.
(28) Bond, A. M.; Henderson, T. L. E.; Mann, D. R.; Mann, T. F.; Thormann, W.; Zoski, C. G. *Anal. Chem.* **1988**, *60*, 1878.
(29) Levine, I. N. *Physical Chemistry*, 5th ed.; McGraw-Hill: New York, 2002; p 504.
(30) Flanagan, J. B.; Margel, S.; Bard, A. J.; Anson, F. C. *J. Am. Chem. Soc.* **1978**, *100*, 4248.
(31) Shoup, D.; Szabo, A. *J. Electroanal. Chem.* **1982**, *140*, 237.
(32) Hultgren, V. M.; Mariotti, A. W. A.; Bond, A. M.; Wedd, A. G. *Anal. Chem.* **2002**, *74*, 3151.
(33) (a) Roe, D. K.; Toni, J. E. A. *Anal. Chem.* **1965**, *37*, 1503. (b) de Vries, W. T.; van Dalen, E. *J. Electroanal. Chem.* **1964**, *8*, 366. (c) Shain, I.; Lewinson, J. *Anal. Chem.* **1961**, *33*, 187.
(34) Amatore, C.; Saveant, J. M.; Tessier, D. *J. Electroanal. Chem.* **1983**, *147*, 39.
(35) (a) Kralj, B.; Dryfe, R. A. W. *Phys. Chem. Chem. Phys.* **2001**, *3*, 5274. (b) Josserand, J.; Morandini, J.; Lee, H. J.; Ferrigno, R.; Girault, H. H. *J. Electroanal. Chem.* **1999**, *468*, 42. (c) Wilke, S.; Zerihun, T. *Electrochim. Acta* **1998**, *44*, 15.
(36) Bond, A. M.; Marken, F. *J. Electroanal. Chem.* **1994**, *372*, 125.
(37) Bard, A. J.; Fan, F. R.-F.; Mirkin, M. V. In *Electroanalytical Chemistry*; Bard, A. J., Ed.; Marcel Dekker: New York, 1994; Vol. 18, p 243.
(38) Schröder, U.; Oldham, K. B.; Myland, J. C.; Mahon, P. J.; Scholz, F. *J. Solid State Electrochem.* **2000**, *4*, 314.
(39) Lee, W. Y.; Majda, M.; Brezesinski, G.; Wittek, M.; Mobius, D. *J. Phys. Chem. B* **1999**, *103*, 6950.
(40) Hubbard, A. T.; Anson, F. C. In *Electroanal. Chem.*; Bard, A. J., Ed.; Marcel Dekker: New York, 1970; Vol. 4, p 129.
(41) Nicholson, R. S.; Shain, I. *Anal. Chem.* **1964**, *36*, 706.
(42) Britz, D. *Digital Simulation in Electrochemistry*, 2nd ed.; Springer-Verlag: New York, 1988.
(43) Feldberg, S. W. *J. Electroanal. Chem.* **1981**, *127*, 1.